Water Research X 30 (2026) 100466

Contents lists available at ScienceDirect

Water Research X

journal homepage: www.sciencedirect.com/journal/water-research-x

Urban blocks enable data-reduced, hydraulically sound planning for combined sewer overflow mitigation

Daneish Despot *, Ganbaatar Khurelbaatar, Maria Chiara Lippera, Snigdha Dev Roy, Roland Müller, Jan Friesen

Department of Systemic Environmental Biotechnology, Helmholtz Centre for Environmental Research—UFZ, Permoserstrasse 15, 04318 Leipzig, Germany

ARTICLE INFO

Keywords:
Combined sewer overflows
Stormwater management
Data-reduced
Block-scale planning
Network generation

ABSTRACT

Combined sewer overflows (CSOs) remain a major source of urban water pollution, exacerbated by increasing rainfall extremes and expanding impervious surfaces. Yet efforts to model and mitigate CSOs are often hampered by limited access to detailed sewer infrastructure data. This study presents a data-reduced modelling framework based on delineated urban blocks, which serve as both hydrological response units and the spatial basis for generating gravity-consistent synthetic sewer networks from open geospatial data. We compared four model configurations: Thiessen polygons with a real network, blocks with a real network, blocks with a synthetic network, and a lumped model, using 32 monitored overflow events in a Swiss catchment. The synthetic block model reproduced overflow volumes within –10 % to +20 %, matched 80 % of peak timings within 15 min, while reducing structural complexity by approximately 30 %. Kling–Gupta efficiency scores confirmed valid performance, though simplified models tended to overpredict peak flows and underestimate overflow durations. The synthetic configuration exhibited more frequent surcharging and lower conduit storage near the outlet, reflecting geometric trade-offs in the automated layout. Despite these limitations, block-based models preserve spatial attribution of runoff and enable rapid screening of decentralised interventions without requiring full network datasets. The framework supports early-stage planning and is compatible with both open-source and utility-held data. By aligning model structure with urban form and reducing data demands, this approach offers a scalable, reproducible framework for planning and prioritising decentralised interventions for CSO mitigation, even in cities with limited access to sewer infrastructure data.

1. Introduction

Combined sewer systems (CSS), introduced in the mid-nineteenth century to protect public health, still serve many modern cities as single-pipe systems to convey both wastewater and stormwater to treatment plants (Butler et al., 2018; Tibbetts, 2005). Even during common storm events, these systems can become overloaded, triggering overflows at designated relief points—combined sewer overflows (CSOs)—or through manholes, which remain a major contributor to urban water pollution despite stormwater dilution (Petrie, 2021; Phillips et al., 2012). Urbanisation and climate change intensify this challenge: the expansion of impervious surfaces increases runoff volumes, while shifts in rainfall patterns, including more frequent short, intense bursts, can push many systems beyond their intended operating range (Angel, 2023; Farina et al., 2024; Fowler et al., 2021). Regulatory standards have tightened internationally; for example, the revised 2024 EU Urban Wastewater Treatment Directive sets a non-binding target to limit storm overflows to ≤2 % of annual dry-weather load, while the U.S. policy similarly enforces controls under the CSO Control Policy and Water Infrastructure Act (European Parliament and Council of the European Union, 2024; United States Congress, 2019; United States Environmental Protection Agency, 1994). Despite these efforts, infrastructure once built to protect public health still pollutes urban waterways, underscoring the need for planning tools that help cities evaluate decentralised stormwater interventions and reduce pressure on centralised systems.

Cities increasingly rely on decentralised stormwater measures to reduce surface runoff entering combined sewer systems and improve urban water resilience. Low Impact Development (LID) approaches are one such measure that introduce infiltration and storage features into the urban fabric to retain runoff near its source (Friesen et al., 2025; Martin-Mikle et al., 2015; Wright et al., 2016). Supporting such

* Corresponding author.
E-mail address: daneish.despot@ufz.de (D. Despot).

https://doi.org/10.1016/j.wroa.2025.100466
Received 11 September 2025; Received in revised form 8 December 2025; Accepted 9 December 2025
Available online 10 December 2025

interventions requires planning tools that can represent spatial variability in runoff generation at appropriate scales. However, many existing planning tools face practical limitations when applied to this context: they require detailed input data due to high data demands, lack spatial explicitness, are difficult to reproduce with open datasets, and often prioritise detailed simulation over usability (Bach et al., 2020; Duque et al., 2022; Kuller et al., 2022, 2017; Rauch et al., 2017).

For CSO mitigation in particular, planning tools require an understanding of how surface runoff is routed through sewer networks, yet available modelling approaches fall at opposite ends of the spectrum. Detailed urban drainage models, such as the U.S. Environmental Protection Agency (EPA) Stormwater Management Model (SWMM), provide comprehensive representations of runoff generation and hydraulic routing (Rossman, 2010), but require extensive input data and high computational effort, which limit their use in early-stage planning (Chegini et al., 2025). Network simplification strategies—including conduit pruning, subcatchment aggregation, and network skeletonisation—reduce model resolution but still depend on surveyed sewer networks and case-specific assumptions (Cantone and Schmidt, 2009; Goldstein et al., 2016; Krebs et al., 2014; Pichler et al., 2024). At the opposite extreme, hydrological simplification approaches omit the sewer network entirely and rely on lumped or data-driven formulations that estimate overflows using proxy variables such as imperviousness, rainfall, or population (Farina et al., 2023; Montoya-Coronado et al., 2024; Quaranta et al., 2022). Collectively, these detailed and highly simplified approaches leave a clear methodological gap: a simple, spatially explicit, open-data modelling framework that retains essential hydraulic information while remaining compatible with early-stage planning.

Urban blocks represent a practical spatial unit for managing runoff near its source. Defined as the areas enclosed by bordering streets, they represent the essential intermediate scale of urban form that aligns closely with how cities organise land use and plan local infrastructure (Conzen, 1960; Moudon, 1997; Oliveira, 2024; Siksna, 1997). Hydrologically, blocks act as relatively uniform runoff units that contribute discretely to the larger catchment. Previous studies support this dual identity—as meaningful units in both urban planning and hydrology: the MUST-B framework demonstrated that blocks can function as the smallest hydrological unit for modelling infiltration and retention (Khurelbaatar et al., 2021), while Lippera et al. 2025 showed their usefulness for identifying areas suitable for decentralised interventions to reduce CSOs. In contrast, conventional subcatchments used in urban drainage models are delineated by drainage connectivity—typically as Thiessen polygons or DEM-based flow areas around manholes (Ji and Qiuwen, 2015; Si et al., 2024), which represent purely hydrologic aggregation units disconnected from the urban structure. To our knowledge, no study has examined whether block-based units can reproduce the hydrologic response of conventional subcatchments or explored how block boundaries can support the derivation of drainage inlet points and the generation of a synthetic sewer network directly from open geospatial data. This gap highlights the potential of urban blocks to bridge urban morphology and drainage modelling, particularly for planning decentralised interventions.

We propose a data-reduced, block-based modelling workflow that uses open geospatial data to support early-stage evaluation of combined sewer overflow (CSO) risk. In this framework, urban blocks serve two complementary roles: (i) as hydrological response units aligned with planning needs, and (ii) as geometric outlines for generating synthetic, gravity-prioritised sewer networks in the absence of detailed sewer asset data. We implement this capability by automatically linking each block to a drainage inlet and generating a network layout from street-network and elevation data, following graph-based hydraulic principles demonstrated in open-source tools, such as pysewer, REWATnet, and SWMManywhere (Calle et al., 2023; Dobson et al., 2025; Sanne et al., 2024).

Our central question is: To what extent can urban blocks be used to simplify urban drainage models, both spatially and hydraulically, without compromising key CSO behaviours and network performance? To answer this, we evaluate four model configurations across a gradient of data complexity: a conventional model setup—the reference model, two block-based setups (using real and synthetic sewer networks), and a lumped alternative. We address this through three objectives:

1. Assess model accuracy under different spatial and hydraulic simplifications using cross-validation across 32 storm events.
2. Evaluate network-level hydraulic performance using indicators such as the Hydraulic Performance Index (HPI) and Contributing Area Impact (CAI).
3. Examine CSO behaviour across configurations, focusing on reliability, reproducibility, and suitability for decentralised planning.

Overall, we aim to assess whether data-reduced, block-based models can reproduce key CSO dynamics with sufficient reliability for early-stage planning, and to clarify the trade-offs introduced by spatial and hydraulic simplification.

2. Materials and methods

2.1. Case study and monitoring data

To evaluate how spatial and hydraulic simplification affects CSO modelling, we tested four configurations in a real-world case study, including a conventional configuration and two block-based variants, as well as a lumped alternative. The study area used was a 16.85-hectare industrial CSO catchment (RÜB Industrie, RUB80) in Fehraltorf, about 15 km east of Zürich, Switzerland. As part of the Urban Water Observatory (UWO) initiative, the site provides high-resolution, open-access data, including a full SWMM model (the original model) and hydrological and meteorological observations, offering a controlled sandbox for developing and verifying the data-reduced modelling concept presented in this study. (Blumensaat et al., 2022a, 2022b, 2023b). The CSO catchment receives dry-weather inflow equivalent to approximately 981 inhabitants and surface runoff from 7.6 hectares of impervious area draining to a 200 m^3 flow-through storage basin equipped with a pump station (Blumensaat et al., 2023a). Under dry weather conditions, flows are pumped to the wastewater treatment plant; during rainfall, excess water is discharged to the Kempt River via the monitored weir (Fig. 1). Despite its small size, the area contributes 10–15 % of the annual CSO volume at the catchment scale, confirming its hydraulic relevance (Rodriguez et al., 2024).

For this study, rainfall and combined sewer overflow observations from 2019 to 2020, recorded at a 1-minute temporal resolution, were used to identify calibration and validation events. Rainfall events were defined as continuous periods with an intensity >0.1 mm/h, separated by at least 6 h of no rain (inter-event dry period) (Broekhuizen et al., 2020). Overflow events were identified when discharge exceeded 0.1 L/s and were merged if interruptions $\leq$ 3 h occurred to preserve hydraulic continuity and avoid splitting a single overflow response caused by regulator behaviour or sensor noise. Each overflow was then linked to a storm if it started within 6 h after the rainfall began, ensuring one overflow per storm event. In total, 32 observed events met these criteria and were used for model calibration and testing. For each event, we calculated rainfall duration, depth, and intensity, overflow volume and duration, lag time and antecedent dry period (ADP). A summary of rainfall event characteristics is provided in Supplementary Table ST2. Event severity was classified using Intensity–Duration–Frequency (IDF) curves (DWA-A 531, 2025) derived from a 35-year, 10-minute rainfall series recorded at a station 15 km from Fehraltorf (MeteoSwiss, 2024).

2.2. Urban block mapping

Urban blocks were delineated from the OpenStreetMap (OSM) street

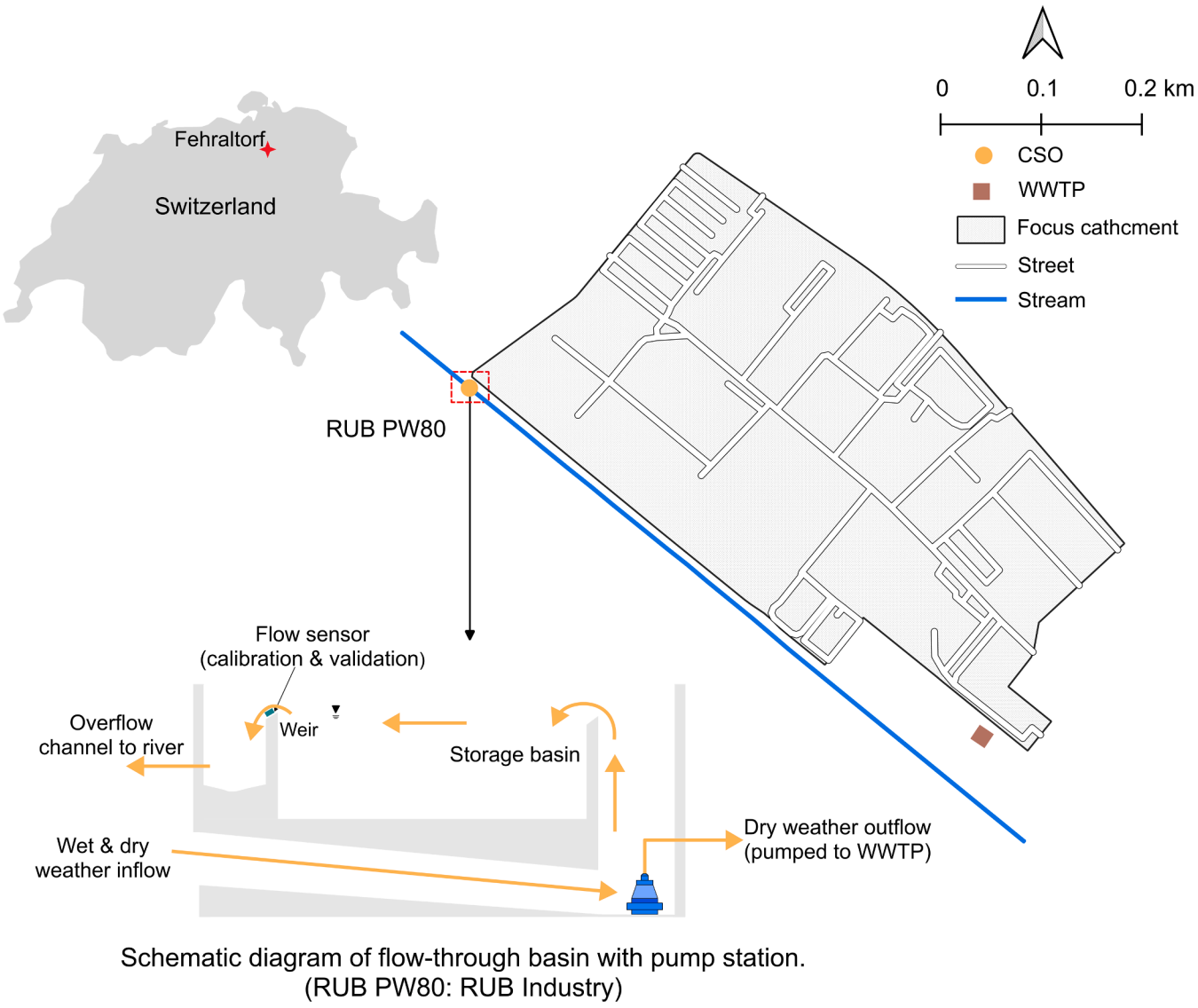

Fig. 1. Overview of Fehraltorf's industry combined sewershed, located near Zurich, Switzerland. The study focuses on a 16.85-hectare industrial CSO catchment (shaded), draining to the RÜB Industrie overflow structure.

network using OSMnx (Boeing, 2025). The street-network graph was simplified to remove artefacts such as isolated links, dead-end nodes, and to consolidate intersections, ensuring topological consistency. Blocks were then derived by converting cleaned street centerlines into closed polygons, assigning half the street width to each side so that rights-of-way were fairly distributed among adjacent blocks. This approach ensured geometric alignment between street layouts and block boundaries, producing spatially coherent hydrological response units.

Block attributes were calculated using multiple open data sources. Slope was derived from the UWO digital elevation model (DEM), while imperviousness was computed using the World Settlement Footprint (WSF 2019) raster (German Aerospace Center, 2023). The raster was clipped to block extents and sealed pixels vectorised, allowing impervious area to be calculated as the ratio of sealed to total block area. Dry-weather flow for each block was assigned using the inflow values defined by the catchment characteristic, while groundwater infiltration was distributed proportionally to match the observed total inflow conditions represented in the original UWO model. Additional geometric properties, such as block area and characteristic width, were computed to support hydrological parameterisation. Width was calculated as the area divided by convex-hull diameter (D_p), representing the block's longest internal span. This setup provided each block with hydrologically meaningful attributes while remaining fully automatable with open geospatial data.

2.3. Synthetic sewer network

To represent drainage networks in data-scarce contexts, a synthetic combined sewer network was generated using the open-source Python package pysewer (Sanne et al., 2024). This method produces topologically valid, gravity-driven sewer networks using elevation data, road layouts, and building locations. For this study, we adapted pysewer to work with block geometries and to represent combined sewer flow conditions, including both dry- and wet-weather components. This method provides a quick, consistent framework for generating sewer network layouts that reflect the typical alignment and structure of real urban drainage systems, supporting exploratory analyses for planning applications.

Block connection manholes (drainage inlets) were used as network nodes and assigned the aggregated inflow attributes of the contributing blocks. Wet-weather contributions were represented indirectly through a combined-sewer factor (equivalent to the traditional dilution factor),

which scales dry-weather inflows by a uniform wet-to-dry ratio. This factor was iteratively adjusted until the total storage volume of the synthetic network matched that of the real system, ensuring comparable hydraulic behaviour while maintaining data reduction.

The synthetic network was constructed as a directed graph, with nodes representing manholes and conduits representing sewer sections. A repeated shortest-path heuristic was applied using manhole connection points to generate a directed Steiner arborescence (Hwang and Richards, 1992) to route flows toward the CSO control structure, ensuring gravity-driven routing and minimising unrealistic loopbacks. Conduit diameters were sized based on blocks' dry-weather peak inflows scaled by the combined sewer factor. Trench invert elevations were derived from the DEM using trench depth limits of 1–8 m and a minimum slope constraint of −0.01. The conduit slope was calculated as the average invert slope between the upstream and downstream trench elevations of each conduit. This workflow created a simplified network based on block outlines, approximating the gravity-driven routing and storage capacity of the real drainage system.

2.4. Connection manholes

To assign subcatchments to the connection manholes, we implemented two methods designed for different data scenarios.

1. **Frontage buffer method:** Used when connecting to known manholes (invert elevation available). Blocks were buffered by 10 m to approximate the typical placement of manholes along the public right-of-way. Manholes intersecting this zone were identified using a spatial index, and the one with the lowest invert elevation was selected. This improves on typical centroid-based linking approaches, which often assign subcatchments to the nearest node using Euclidean distance or simple snapping, without considering topographic or urban form constraints (Schilling and Tränckner, 2022; Si et al., 2024).
2. **Road-profile method:** Developed for synthetic network applications where explicit manhole data are unavailable. Road elevations were sampled from the DEM at 10-m increments around each block, and the lowest point sampled was assigned the virtual connection manhole. To avoid overloading a single inlet point, the reuse of manholes was limited to three blocks per manhole. Finally, if a block corner (junction) was found within 30 m of the candidate manhole and had a similar elevation (within 0.5 m), the outlet was snapped to that junction, while ensuring 80 m manhole spacing was maintained. This ensured that connection manholes remained topographically plausible and aligned with the block boundary.

These connection methods are depicted in Supplementary Figure SF5.

2.5. Model configurations

We assembled four configurations that represent distinct positions along a gradient of spatial and hydraulic simplification (Fig. 2). All four configurations shared identical rainfall input, groundwater infiltration, dry-weather flow, and CSO control structure (200 m^3 basin, pump station, and overflow weir; Fig. 1). This ensured that differences in results could be attributed solely to differences in surface discretisation and network representation. Each configuration is briefly described below.

1. Thiessen: $Real_{net}$

Subcatchments were delineated using Thiessen polygons around observed manholes, following the standard approach in SWMM practice when detailed surface delineations are unavailable. These polygons were then connected to the surveyed sewer network, preserving the real pipe layout, invert elevations, and control structures. This configuration

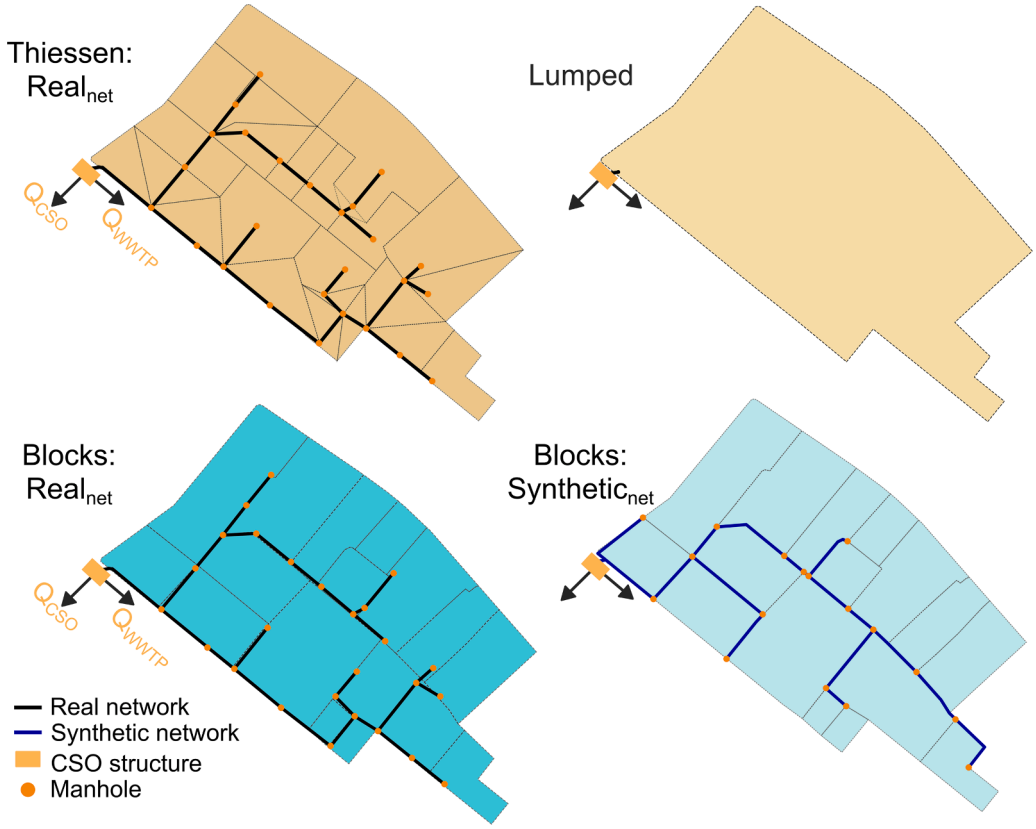

Fig. 2. Schematic of the four model configurations tested: Thiessen: $Real_{net}$, Blocks: $Real_{net}$, Blocks: $Synthetic_{net}$, and Lumped. All share identical rainfall forcing and CSO control structure but differ in surface discretisation and network representation.

represents the planning-level reference model against which alternatives were compared.

2. Blocks: $Real_{net}$

Urban block polygons served as subcatchments, linked to the sewer network via the frontage buffer method. While the network topology and conduit characteristics were identical to Thiessen: $Real_{net}$, the surface discretisation was fundamentally different, reflecting the block-based approach introduced in this study.

3. Blocks: $Synthetic_{net}$

Blocks were connected using the road-profile method to a synthetic network generated with pysewer (see 2.3 Synthetic sewer network). The generated network preserved topological validity and generalised gravity-driven routing, but differed from the surveyed network in pipe lengths and diameters.

4. Lumped

A single subcatchment aggregated the entire sewershed area and drained directly to the CSO structure, with dry-weather flow and infiltration scaled accordingly. The internal network was reduced to a minimal representation, with no distributed routing or intermediate nodes. This setup represents the extreme simplification of both hydrological and hydraulic detail.

Table 1 summarises the four model configurations analysed in this study, highlighting the main model components and corresponding evaluation aims.

2.6. Overview of evaluation objectives and indicators

To evaluate how structural simplification affects model reliability, we assessed performance across both a data-reduction and structural complexity gradient, ranging from fully detailed to highly simplified configurations. Following James (2000), structural complexity was quantified using a weighted count of SWMM elements, providing context for interpreting trade-offs between model size and fidelity. Further details are provided in Supplementary Note SN1.

Performance indicators were grouped according to three supporting objectives (Table 2). These span: (i) model accuracy (goodness-of-fit), where we quantified predictive skill using Kling–Gupta efficiency (KGE; Gupta et al., 2009) and event-scale error metrics; (ii) network-level hydraulic performance, assessed with indices of stress and load; and (iii) event-scale CSO behaviour, characterised by volume, timing, and detection statistics.

For clarity, we use the following terminology: a node represents a SWMM junction, outfall, or storage (e.g., a manhole or inlet where runoff enters); a conduit is a SWMM pipe element between two nodes. A drainage inlet denotes the node receiving runoff from a block or subcatchment.

Table 1
Overview of model configurations, key components, and evaluation aims.

Model configuration	Model components and specifications	Evaluation aim
Thiessen: $Real_{net}$	Conventional Thiessen-polygons subcatchments coupled with the real (surveyed) sewer network (SN); observed hydrological and site-specific datasets	Reference model for comparison with simplified configurations.
Blocks: $Real_{net}$	Subcatchment delineation based on urban blocks derived from open geospatial datasets; real SN; observed hydrological and site-specific datasets	Assess effect of spatial discretisation. (Blocks vs Thiessen polygons)
Blocks: $Synthetic_{net}$	Subcatchment delineation based on urban blocks derived from open geospatial datasets, use of synthetic SN; observed hydrological, site-specific datasets,	Evaluate whether blocks and sewer networks derived from open geospatial data can reproduce CSO dynamics where no surveyed SN data are available.
Lumped	Single aggregated subcatchment without a sewer network	Establish lower-bound performance sensitivity to complete structural simplification.

Table 2
Overview of the indicators used to assess model performance with respect to the outlined research objectives.

Objective	Indicators	Definition/ Note
(i) Model accuracy along data-reduction gradient	Raw KGE; Normalised KGE (KGE × acceptance rate, threshold KGE ≥ 0.2); Overflow volume error (%); Peak flow error (%); Time-to-peak error (min)	KGE compares correlation, bias, and variability between simulated and observed CSO discharge; event-scale errors quantify accuracy of specific hydrograph features.
(ii) Network-level hydraulic performance	Hydraulic Performance Index (HPI); Contributing Area Impact (CAI); CSO attribution; Flow Instability Index (FII)	HPI: surcharge relative to burial depth (%). CAI: upstream load share (%). Critical conduits defined by HPI ≥ 60 and CAI ≥ 75.
(iii) Event-scale CSO behaviour	Overflow volume classification; Peak discharge distribution; Overflow duration distribution; Spill frequency; Detection rate; Error direction	Derived from event-scale simulations, compared with 32 observed events. Captures whether simplified models reproduce the magnitude, timing, and frequency of CSO events.

2.7. Multi-event calibration and validation

To evaluate parameter sensitivity, we first applied a variance-based sensitivity analysis using Saltelli sampling ($N = 1024$) (Saltelli, 2002; Sobol′, 2001), focusing on total outflow and peak flow as model responses. The most influential parameters were imperviousness, impervious depression storage, Manning's roughness for impervious areas, subcatchment width, conduit slope, and conduit roughness. These parameters were retained for calibration.

To evaluate the robustness and generalisability of each model configuration, we applied a five-fold cross-validation framework inspired by standard practices in machine learning model assessment (Stone, 1974). In each fold, 80 % of observed events were used for calibration and 20 % for validation. Calibration was performed using the Shuffled Complex Evolution algorithm (SCE-UA) (Duan et al., 1994), as implemented in the SPOTPY package (Houska et al., 2015). Parameters were sampled from uniform distributions within bounds derived from the sensitivity analysis. The Kling-Gupta efficiency (KGE) was used as the sole objective function, with a behavioural threshold of KGE ≥ 0.2. Each calibration run was limited to 25,000 evaluations, with early stopping if convergence criteria were met. Across all folds and models, this yielded roughly 500,000 simulations.

Model fidelity was assessed using the Kling–Gupta Efficiency (KGE), supported by event-scale errors in overflow volume (%), peak discharge (%), and time-to-peak (minutes). To justify the performance ranges used in this study (Knoben et al., 2019), KGE values were compared with these hydrological error metrics against accepted ranges for urban drainage modelling (volume error:10 % to +20 %; peak error:15 % to +25 %; James, 2000). These thresholds correspond to performance typically considered sufficient to inform planning and scenario screening, rather than for detailed hydraulic design. This analysis revealed consistent clustering patterns, informing a classification scheme: "Poor" (KGE < 0.2), "Acceptable" (0.2–0.5), "Good" (0.5–0.7), and "Very Good" (KGE ≥ 0.7), as exemplified in Supplementary Figure SF1, which compares KGE values with overflow volume and peak errors. Simulations achieving KGE ≥ 0.2 were classified as behavioural—model runs that adequately reproduce the observed system response within the derived KGE threshold (Beven and Binley, 1992). The corresponding behavioural parameter sets were then used for subsequent

analysis.

For each fold, the median of all behavioural parameter sets from the training phase was selected as the representative parameter set, which was then applied to the associated test events. This constituted the test phase of the cross-validation framework, which primarily evaluated model generalisability. Model performance was evaluated per test event and aggregated across folds using KGE, normalised KGE, event rejection rate (proportion of test events with KGE < 0.2), and the previously defined error metrics.

To assess differences between model configurations, non-parametric statistical tests were applied. The Kruskal–Wallis H test was used to assess overall differences in KGE and normalised KGE, and Mann–Whitney U tests were applied for pairwise comparisons between reference or lumped models and the block-based alternatives.

Finally, a global parameter set was derived by pooling all valid parameter sets (KGE ≥ 0.2) from the training phases of all folds and computing their median. This aggregated set was then applied in full-domain simulations to assess combined sewer overflow (CSO) dynamics and hydraulic performance under representative conditions. Parameter bounds and uniform distributions used in calibration are listed in Supplementary Table ST4.

2.8. Network and CSO performance metrics

Performance was evaluated at both the external CSO scale and the internal network scale using a combination of indices and graph-based tracing methods.

The Hydraulic Performance Index (HPI) quantified conduit stress as the ratio of surcharge height above the pipe crown to burial depth, expressed as a percentage. Conduits without surcharge (free surface flow conditions) were assigned an HPI of 0, while 100 % indicates when the surcharge reaches ground level. Conduits with an HPI $\geq$ 60 % were considered critically stressed.

To determine a subcatchment's contribution to CSO, we assessed whether the subcatchment's outlet node has a directed path to the CSO node within the sewer network graph. Subcatchments with a reachable path were included in the contributor set $\mathscr{U}_c$. The relative contribution of each subcatchment was then calculated as:

$$C_i = 100 \times \left(\frac{V_i}{\sum_{j \in \mathscr{U}_c} V_j} \right)$$

Where V_i denotes the total runoff volume from the subcatchment i during the storm event. Subcatchments with no downstream path to the CSO node or with a zero-runoff volume were assigned a zero contribution, ensuring that only hydraulically connected areas were considered.

The Contributing Area Impact (CAI) captured load accumulation by tracing runoff propagation through the network. CAI for each conduit was defined as a volume-weighted flow accumulation index (Beven and Kirkby, 1979; Reyes-Silva et al., 2020). For each subcatchment, all conduits downstream of its outlet were identified, including the initial pipe segment and its runoff volume. Repeating this for all subcatchments yielded total accumulated volumes per conduit. CAI for conduit k was then expressed as:

$$\mathrm{CAI}_k = 100 \times \frac{\sum_i 1(i \to k) \cdot V_i}{\max_m \left(\sum_i 1(i \to m) \cdot V_i \right)}$$

where $1(i \to k)$ is an indicator equal to 1 if pipe k lies on a downstream path from subcatchment i, and 0 otherwise. This metric identifies accumulation hotspots and potential bottlenecks, relative to the most loaded conduit.

Plotting HPI against CAI for all conduits enabled classification into stable, stressed, loaded, or critical categories, highlighting bottlenecks and stress patterns. These two indices formed the core of our hydraulic evaluation. Additional diagnostics, including the Flow Instability Index (FII), conduit storage, and monotonic upsizing checks, are provided in Supplementary Note SN3.

At the CSO scale, we reported overflow volume, peak discharge, and duration. Events were deemed valid if they met the KGE threshold of $\geq$ 0.2. Spill frequency, detection rates, and error direction (over- vs underestimation) were also analysed. To interpret event-scale overflow-volume errors, simulated volumes were classified as Good (<15 %), Acceptable (15–30 %), or Poor (>30 %), consistent with recommended tolerances typically used in urban drainage modelling (James, 2000).

2.9. Modelling framework and automation

All simulations were carried out with the U.S. EPA Storm Water Management Model (SWMM), using the dynamic-wave solver to account for surcharging, backwater effects, and flow reversals (Rossman, 2017). The workflow was automated in Python, with swmm-api (Pichler, 2025) used for input file manipulation and result extraction, pysewer (Sanne et al., 2024) for synthetic network generation, SALib (Herman and Usher, 2017), for sensitivity analysis, SPOTPY (Houska et al., 2015) for calibration, and NetworkX (Hagberg et al., 2008) for graph-based diagnostics. Statistical analyses were performed with SciPy (Virtanen et al., 2020). All simulations were carried out on a high-performance computing cluster (See Additional Data). A full list of package versions is provided in Supplementary Table ST10 and Figure SF4, which shows the automated block-SWMM modelling pipeline.

3. Results

3.1. Comparison of performance along a data-reduced gradient

We compared the four model configurations along a gradient of spatial and hydraulic complexity, ranging from the detailed Thiessen: $\mathrm{Real}_{\mathrm{net}}$ (the reference) to the fully aggregated Lumped setup. Relative to the reference, structural complexity was reduced by approximately 12 % in Blocks: $\mathrm{Real}_{\mathrm{net}}$, 28 % in Blocks: $\mathrm{Synthetic}_{\mathrm{net}}$, and 91 % in Lumped, reflecting fewer SWMM elements (subcatchments, nodes, and conduits) while preserving the same hydrologic and hydraulic process representations. The Lumped setup contained nearly one order of magnitude fewer elements than the network-based configurations. The full breakdown of subcatchments, nodes, and complexity scores is provided in Supplementary Table ST1.

Cross-validation results show that all configurations reproduced CSO discharge with comparable overall predictive skill, although their consistency across events differed (Fig. 3). The Lumped model achieved the highest raw KGE scores but had the lowest acceptance rate—fewer than one in four test events exceeded the behavioural threshold (KGE $\geq$ 0.2). Consequently, its normalised KGE, defined as the product of the KGE and acceptance rate, dropped significantly. In contrast, Blocks: $\mathrm{Synthetic}_{\mathrm{net}}$ was the most consistent, yielding the highest number of valid test events and the lowest rejection rate. The Thiessen: $\mathrm{Real}_{\mathrm{net}}$ and Blocks: $\mathrm{Real}_{\mathrm{net}}$ configurations performed intermediately, with fold-level KGE typically ranging from 0.35 to 0.59. Differences in normalised performance were mainly driven by acceptance rates rather than by best-fold outcomes. The Kruskal–Wallis H test indicated no statistically significant differences in KGE across the model configurations (p-value > 0.1), suggesting that, on average, all models reproduced overflow dynamics with comparable predictive skill. Pairwise statistical comparisons are available in Supplementary Note SN2.

Event-scale error metrics further illustrate how simplification affected overflow dynamics. The Lumped model showed the smallest deviations in overflow volume (–12.5 $\pm$ 15.0 %) and peak flow (5.9 $\pm$ 3.6 %), although its time-to-peak error was highly variable (–3.5 $\pm$ 33.3 min). Blocks: $\mathrm{Synthetic}_{\mathrm{net}}$ achieved similar reliability for volume (–20.2 $\pm$ 16.7 %) and time-to-peak (0.5 $\pm$ 13.9 min), but exhibited larger peak errors (38.6 $\pm$ 13.1 %). The Thiessen: $\mathrm{Real}_{\mathrm{net}}$ and Blocks: $\mathrm{Real}_{\mathrm{net}}$ both

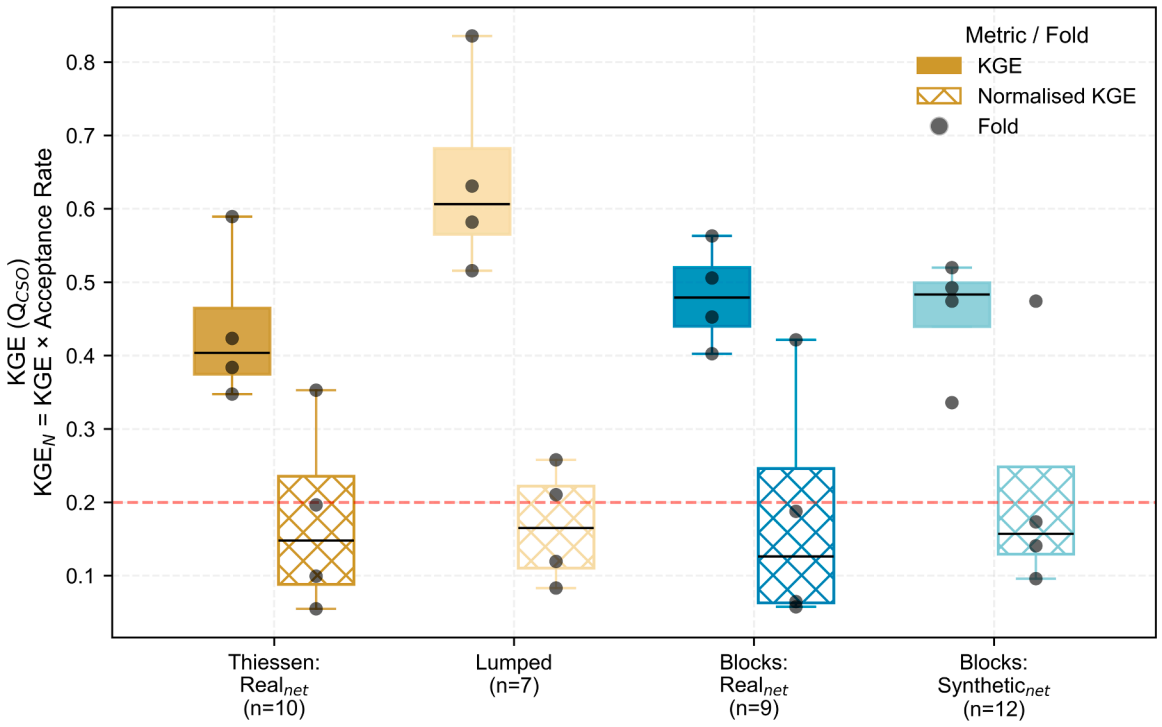

Fig. 3. Cross-validation performance based on raw and normalised Kling–Gupta efficiency (KGE). KGE values are calculated with respect to the CSO discharge (Q_{CSO}). The normalised KGE: KGE × acceptance rate (i.e., the proportion of test events with KGE ≥ 0.2 in each fold). Folds are represented by the black dots (folds with no valid model responses were excluded), with fold-level results derived from simulations of 6–7 test events per fold.

tended to underestimate overflow volumes (−31 % and –34 %), while overestimating peaks (32–34 %). In all network-based models, the peaks were generally too high; however, the timings were within 10 min of the observed events. These results indicate that simplification primarily affects error direction and consistency across events, while overall model performance remains comparable.

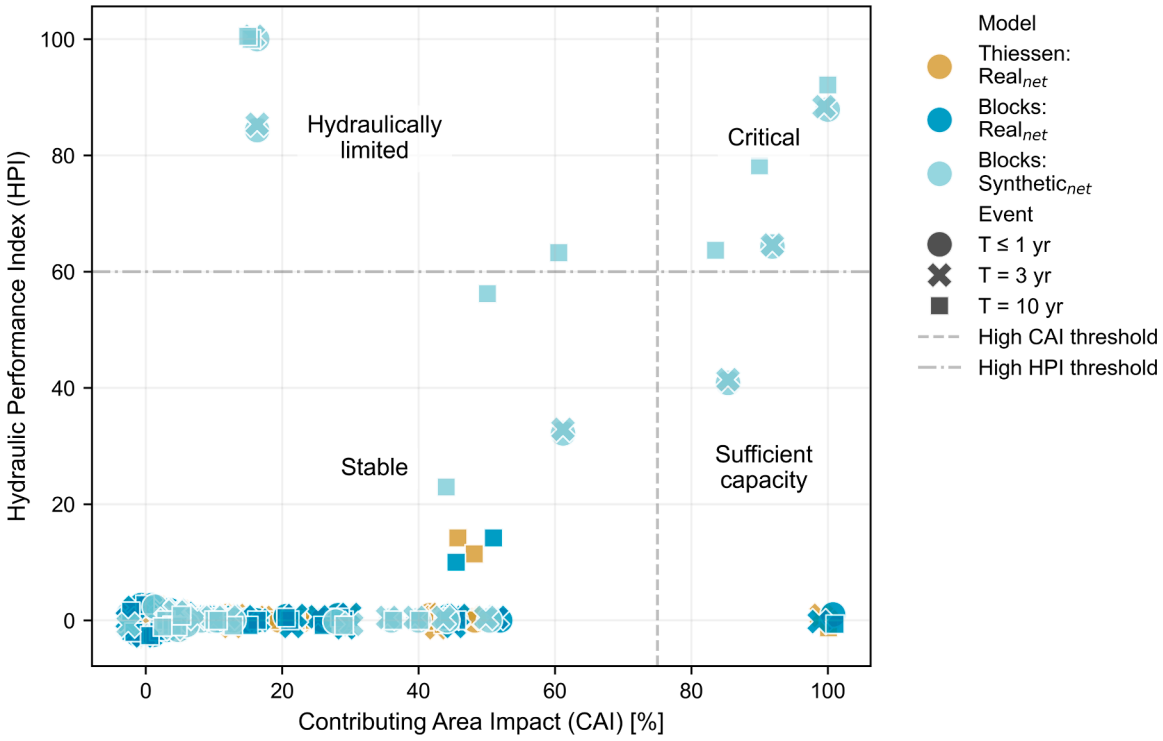

Fig. 4. Conduit-level HPI–CAI scatter by model and storm class. Each point is a conduit; colours denote model configuration, and markers show storm return periods: $T \leq 1$ yr, $T = 3$ yr, $T = 10$ yr (duration: 5–6 h). The vertical line marks CAI = 75 % (high load) and the horizontal line marks HPI = 60 % (high stress); points in the upper-right are both high-load and high-stress. HPI = Hydraulic Performance Index (surcharge relative to burial depth, %), CAI = Contributing Area Impact (upstream load share, %). Markers are shown with a small positional offset to reveal overlaps; all thresholds and statistics use the original values.

3.2. Impact of the block-based delineation and network simplification on the hydraulic performance

Differences in network representation strongly influenced hydraulic behaviour. Plots of conduit stress (Hydraulic Performance Index, HPI) versus load accumulation (Contributing Area Impact, CAI) revealed clear contrasts between the real and synthetic layouts (Fig. 4). In the Thiessen: $Real_{net}$ and Blocks: $Real_{net}$ configurations, conduits clustered almost entirely in the stable quadrant, with median HPI values close to zero and few conduits exceeding the 60 % surcharge threshold. High-load conduits (CAI $\geq$ 75 %) were rare, and no flooding was observed. Stress and load remained broadly distributed across the network, with attenuation capacity concentrated near the inlet of the CSO control structure, indicating a hydraulically coherent system.

The block-based with the synthetic network displayed markedly different behaviour. Roughly one-quarter of conduits exceeded the 60 % HPI threshold under frequent storms ($T \leq 1$ year, 6 h), increasing to one-third under rarer 10-year return events. Several nodes flooded, and conduits with CAI $\geq$ 75 % were concentrated near the outlet, with a median CAI of 16.3 % compared to 10.9 % in the real block network. As shown in Fig. 4, conduits in the synthetic network shifted toward the high-stress and high-load region with increasing storm severity, whereas the real-network models remained largely stable.

Spatial diagnostics reinforced these findings. Maps of HPI and CSO attribution (Fig. 5) illustrated that surcharge in the real networks was dispersed across upstream reaches, while attenuation potential accumulated in the outlet zone (the last 300 m before the outlet), where 490.2 m^3 of conduit storage was available. By contrast, the synthetic layout exhibited shallower cover depths near the outlet (+3.2 m vs. a median outlet cover depth of −2.6 m in the real network). The synthetic network provided only 351 m^3 of conduit storage, 139.2 m^3 less than the real network, mainly due to the smaller pipe diameters concentrated in the outlet zone. These deficiencies resulted in a concentration of surcharge and high loads directly upstream of the CSO structure, co-located with the subcatchments contributing the largest CSO volumes. The flooded node volume reached 361 m^3 in the synthetic network during the 10-year storm, whereas no flooding occurred in either of the real-network configurations. These diagnostics highlight that the synthetic layout concentrated hydraulic stress in the outlet zone, whereas the real-network configurations distributed it more broadly. Supporting network diagnostics are given in Supplementary Tables ST7–9.

3.3. Assessment of event-based replication of CSO behaviour

Fig. 6 summarises how well each configuration reproduced observed CSO dynamics across 32 events from 2019 to 2020. The Lumped configuration produced the largest share of "Good" events (overflow-volume error <15 %, 28.1 %), followed by the Thiessen reference (25 %). Both block-based configurations captured event dynamics but more frequently fell into the "Poor" category (>30 % error; 72–75 % of events). The error direction was systematic: the Lumped model consistently overestimated volumes, whereas the network-based configurations underestimated (Fig. 6a-b). Spill-frequency and detection-rate indicators showed the same pattern: simulated event counts ranged from 26 in the block-based models to 29 in Lumped, with detection rates highest for Lumped (90.6 %) and lowest for the block-based models (81.2 %).

Peak discharge and overflow duration exhibited consistent biases across configurations (Fig. 6c–d). All models overpredicted peak flows and underestimated long durations. At the 90th percentile, observed

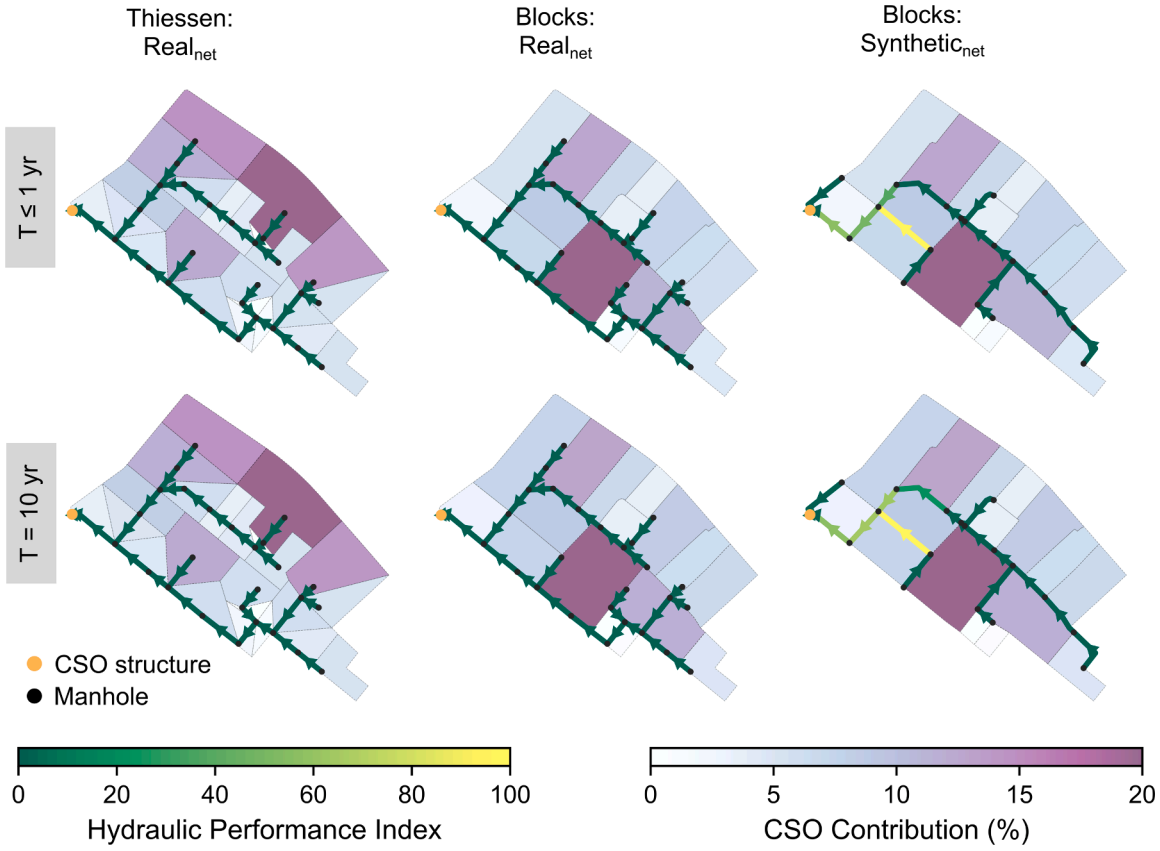

Fig. 5. Maps of Hydraulic Performance Index (HPI) and subcatchment combined sewer overflow (CSO) contribution for two storm classes ($T \leq 1$ year, $T = 10$ year). Subcatchments shading indicates relative CSO contributions (% of total overflow volume) while conduits are coloured based on their hydraulic performance, highlighting regions of significant stress and potential surcharging. Blocks: $Synthetic_{net}$ shows that pipes are undersized near the outlet. Thiessen: $Real_{net}$ shows an unrealistic spatial distribution of total inflow (combined dry- and wet-weather contributions).

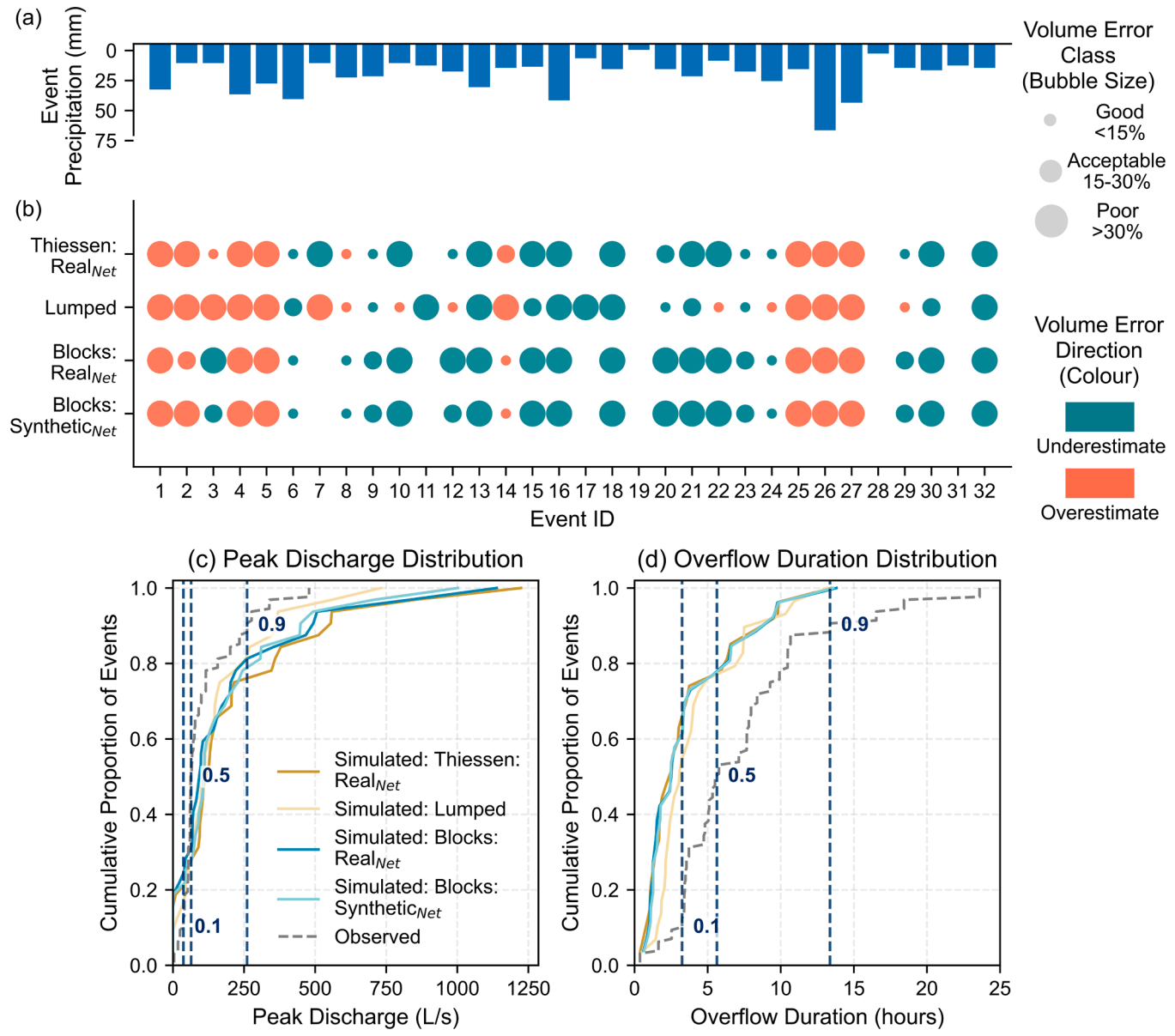

Fig. 6. Event-scale evaluation of overflow dynamics. (a) Event precipitation depth. (b) Overflow volume errors for each model configuration across 32 events, with bubble size indicating error class (<15 % = Good; 15–30 % = Acceptable; >30 % = Poor) and colour showing error direction (■= underestimate, ■= overestimate). (c) Cumulative distribution of simulated versus observed peak discharges—all models overestimate peak flow, reflecting limited flow attenuation and storage effects (subcatchment and network). (d) Cumulative distribution of simulated versus observed overflow durations—shorter simulated duration because delayed drainage and lagged inflow are represented.

peak discharge was 258 L/s, compared to 350 L/s in the Thiessen model and 448–488 L/s in the block-based setups. In contrast, the Lumped configuration aligned with the observed median but still overshot higher percentiles. Overflow durations showed the opposite trend: observed events exceeded 13 h at the 90th percentile, whereas simulated durations ranged from 8 to 9 h. Median durations clustered between 2.5 and 3.1 h, well below the observed 5.6 h. Overall, the network-based models produced shorter hydrographs, while the Lumped setup better approximates duration but fails to reproduce extremes.

Model performance varied further with storm characteristics. Under moderate-depth rainfall (15–45 mm), all configurations produced relatively small biases, whereas high-depth storms yielded larger spreads, with the block-based setups tending to overestimate volumes. Events following long antecedent dry periods (> 24 h) were reproduced more reliably, while those with short dry periods showed wide variability. Infrequent storms (T > 1 yr, 6 h) were the most difficult to capture, showing wide interquartile ranges and frequent overestimation. These findings indicate that event-scale uncertainty increases under extreme or transitional conditions, even when global parameter sets are applied. The detailed event-by-event classification, including how volume error varied with rainfall depth, antecedent dry period, and return period, is provided in Supplementary Figure SF3.

4. Discussion

Urban drainage models are essential tools for mitigating combined sewer overflows (CSOs), but their practical use is often constrained by limited access to detailed network data due to security restrictions, data fragmentation, or incomplete digitisation. This study addresses that challenge by treating urban blocks as dual-purpose units—hydrological response units and structural elements for generating a gravity-consistent synthetic sewer network from open geospatial data. The

resulting block-based workflow aligns both runoff representation and network structure with urban form, enabling complete SWMM model setups when infrastructure datasets are unavailable. Although the study did not simulate specific LID measures, the analyses identified hydraulically stressed and high-impact blocks, indicating where decentralised interventions could be prioritised within the catchment. Among the four configurations, the synthetic block model reproduced overflow volumes within –10 % to +20 %, matched 80 % of peak timings within 15 min, and reduced structural complexity by approximately 30 %. These values fall within accepted performance ranges for urban drainage models, indicating accuracy adequate for comparative CSO screening and early-stage planning. This simplification, however, introduces trade-offs: about one-third of conduits in the synthetic network experienced surcharging, with localised flooding near the outlet, but overall the block-based models maintained reasonable hydraulic performance under strong data reduction.

Cross-validation (CV) results revealed consistent patterns in model calibration and predictive skill. Differences in normalised Kling–Gupta efficiency (KGE) were mainly influenced by the proportion of valid simulations (KGE $\geq$ 0.2) rather than by the best-fold performance, with the synthetic block model achieving the highest share. Predictive skill did not differ significantly across configurations (Kruskal–Wallis, $p >$ 0.1), consistent with homogeneous rainfall forcing that drove similar system responses. Most storms (27 of 32) were frequent ($T \leq 1$ yr) and low-intensity, yet they directly triggered CSOs in this catchment; high-intensity storms were rare. Consequently, calibration reflects behaviour under frequent storms and provides limited insight into rare, intense events. Given the limited storm diversity, these findings elucidate the inherent need for CSO datasets spanning low-, medium-, and high-intensity events to achieve stable, generalisable parameter estimates across conditions. Despite this limitation, consistent structural biases persisted: the Lumped model overestimated overflow volumes, whereas network-based configurations, especially synthetic layouts, underestimated peak discharges and shortened hydrograph tails. Observed flows continued well after rainfall ceased, reflecting delayed drainage and in-pipe storage that are only partly captured in the simplified layouts. Shorter flow paths, reduced conduit storage, and discharge-only calibration therefore yielded sharper runoff responses and faster hydrograph recession. Within the limits of the available dataset, the results indicate that predictive reliability is primarily governed by structural simplification rather than by optimisation constraints.

Network structure strongly shaped model performance. The block-based configurations isolated this effect. Blocks: Real_{net}, which preserved the surveyed network, remained hydraulically stable across storm types. In contrast, the synthetic configuration performed well for frequent to moderate storms but showed increased stress during relatively rare, intense storms. The synthetic network therefore operated largely within its effective range, and its weaker performance under rare extremes reflects structural sensitivity rather than a conceptual inconsistency. Spatial diagnostics confirmed that hydraulic stress in the synthetic layout stemmed not only from smaller conduit diameters but also from geometric and topological trade-offs in the automated layout, including shallow cover depths, minimal detention volume in the outlet zone, and abrupt slope changes at the inlet of the flow control structure. Smaller conduit diameters in the outlet zone further restricted conveyance capacity, amplifying surcharge and localised flooding, as reflected by elevated Hydraulic Performance Index (HPI) values. Similar limitations of synthetic layouts have been noted elsewhere (Chegini and Li, 2022; Dobson et al., 2025; Duque et al., 2022; Ghosh and Hellweger, 2012). Targeted refinements, such as profile smoothing, minimum cover and surcharge constraints (Dobson et al., 2025), or simple outlet-zone detention, can mitigate core limitations without compromising computational effort. Compared with lumped models, which reproduce overall volumes but lack spatial resolution and conduit dynamics (Cantone and Schmidt, 2009; Farina et al., 2023; Goldstein et al., 2016), the block-based framework offers a practical middle ground: it preserves spatial and hydraulic detail necessary to trace conveyance processes while remaining simple enough for automated generation and data-scarce settings.

Beyond standard performance metrics, the models revealed distinct patterns in reproducing CSO behaviour for event volumes, durations, and peak flows. Overflow volumes were generally reproduced within accepted ranges, though network-based configurations tended to underestimate, while the Lumped model showed smaller average biases but with inconsistent direction. Overflow durations were substantially underestimated across all configurations: simulated durations for long events were typically truncated to 8–9 h, whereas observed values exceeded 13 h. These deviations further illustrate how network structure, particularly conduit storage and drainage density, influences both volume and duration, reinforcing the link between structural simplification and modelled CSO behaviour. Reductions in conduit storage suppress hydrograph tails and underestimate cumulative overflow (Supplementary Figure SF2). Conduit storage also influences peak magnitude, with reduced capacity leading to higher simulated peaks (Cantone and Schmidt, 2009). Block-based models consistently overestimated peak discharges (448–488 L/s vs. 258 L/s observed at the 90th percentile), whereas the Lumped configuration matched the median but still overpredicted the upper percentiles. Similar peak inflation has been reported for the same catchment in SuDS scenario modelling (Joshi et al., 2021), indicating that even detailed models face challenges reproducing peak flows. This reflects a well-known trade-off: structural simplification broadens applicability but limits representation of peak-modifying processes, such as detention, surface routing, and flow attenuation (Cantone and Schmidt, 2009). These results emphasise that realistic reproduction of CSO dynamics depends on representing storage and attenuation processes that shape overflow duration and peak control. Addressing these mechanisms—through improved conduit storage representation or coupled surface routing—offers the most direct path to reducing residual biases in simplified models.

Although the block-based framework successfully reproduced baseline CSO dynamics, several limitations should be acknowledged. Stormwater inflows were estimated using a uniform multiplier (combined-sewer factor) applied to dry-weather peaks derived from block-level population estimates that preserved the catchment's population characterisation, rather than computing them directly from impervious area and rainfall. However, because overflow volumes are highly sensitive to impervious-area coverage within each block, this simplification may bias conduit sizing and, consequently, affect overall system capacity. Site-specific factors—e.g., high groundwater infiltration that prolongs hydrograph recession tails (Supplementary Figure SF2)—are only coarsely represented; adding storage or infiltration elements could better represent site-specific drainage behaviour (Blumensaat et al., 2023a; Staufer et al., 2012). While incorporating site-specific factors and detailed engineering design would improve model fidelity, data-reduced methods are inherently unable to capture such fine-scale processes. They will always involve some loss of accuracy.

Furthermore, we evaluated the block-based modelling framework in a small, highly monitored catchment that provided detailed structural information for comparing real and synthetic networks, where frequent storms triggered CSOs. As noted earlier, calibration primarily reflects common storm conditions. Transferability depends on surface and network representation: in dense areas, well-defined streets aid block delineation, but complex surface flow paths, storage, and local drainage features are only approximated; in peri-urban or low-density settings, irregular block boundaries, longer flow paths, higher infiltration potential, and greater depression storage delay and attenuate runoff, potentially requiring adapted delineation or hydrological parameterisation. Synthetic networks generated from open data provide a practical starting point for ungauged or data-poor catchments, but fidelity hinges on assumptions about pipe sizing, runoff, and local detention that vary across cities. Accordingly, while the proposed workflow offers a

useful baseline when surveyed sewer data are unavailable, its uncertainty is likely to increase in areas where rainfall patterns, imperviousness, or drainage layouts differ strongly from those in this study. Together, these factors bound this proof of concept: it demonstrates functional feasibility and identifies where greater physical detail and broader testing are required.

Using urban blocks as the spatial basis for stormwater management provides a practical way to link hydrological modelling with urban planning. Conceptually, the framework is transferable and extensible, as block geometries can be coupled with other hydrologic-hydraulic models or water-quality models and integrated into planning tools to explore green infrastructure options. Future work should refine synthetic network fidelity, expand calibration across various storm conditions and urban settings, and include water quality modules to support source-control assessments.

5. Conclusions

This study demonstrates that urban blocks can serve as hydrologically and hydraulically meaningful spatial units for modelling combined sewer overflows (CSOs), offering a practical middle ground between lumped and survey-dependent reference models. By aligning runoff generation and sewer connectivity with urban form, the block-based framework reproduced key CSO dynamics under frequent storm conditions while reducing structural complexity and data demands by nearly one-third.

Across three objectives—(i) access model accuracy along data-reduction gradient, (ii) evaluate network-level hydraulic performance, and (iii) examine event-scale CSO behaviour, the results show that:

- First, cross-validation across 32 storm events showed that simplified block-based configurations maintained predictive skill comparable to the reference configuration. Systematic biases—volume underestimation and shortened hydrograph tails in network-based setups, and volume overestimation in the lumped model—highlight how structural simplification shapes storage representation and runoff dynamics. These results indicate that meaningful model simplification is achievable while retaining reliable performance under the storm conditions represented in this study.
- Second, network-level evaluation showed that hydraulic stress during more intense storms occurred primarily in the synthetic configuration, where limited conduit storage, shallow cover depths, and smaller pipe diameters in the outlet zone restricted local capacity and increased surcharge potential. In contrast, the Blocks: $Real_{net}$ model remained hydraulically stable across events, demonstrating that urban blocks can function as consistent hydrological units when coupled with a surveyed network, whereas synthetic layouts require further refinement to better represent extreme-event behaviour.
- Third, all configurations reproduced spill frequencies and overflow detection patterns. Block-based models preserved the spatial attribution of contributing areas, linking hydraulic performance to planning and enabling identification of blocks with high potential for decentralised (LIDs) stormwater management or partial disconnection to relieve sewer capacity.

Overall, the block-based framework demonstrates that open and/or minimal datasets can support the setup of hydraulically coherent SWMM models capable of reproducing key CSO dynamics under strong data reduction. While broader testing across diverse storm regimes and urban contexts is needed, the framework provides a transparent and scalable foundation for CSO screening and early-stage planning in settings where detailed networks are limited or unavailable.

Declaration of generative AI and AI-assisted technologies in the writing process

During the preparation of this work, the author(s) used ChatGPT to assist with text reduction, language refinement, and phrasing improvements. After using this tool/service, the author(s) reviewed and edited the content as needed and take full responsibility for the content of the published article.

Additional data

The scientific results have in part been computed at the High-Performance Computing (HPC) Cluster EVE. The main compute hardware of EVE comprises a) 42 compute nodes with dual socket Intel Xeon 6348 CPUs with 512GBs of DDR4 main memory, two of these also include NVIDIA Tesla A100 GPGPUs, and b) 27 compute nodes with dual socket Intel Xeon Gold 6148 CPUs with up to 1536GBs of DDR4 main memory, two of which include NVIDIA Tesla V100 GPGPUs.

CRediT authorship contribution statement

Daneish Despot: Writing – review & editing, Writing – original draft, Visualization, Software, Methodology, Investigation, Formal analysis, Data curation, Conceptualization. **Ganbaatar Khurelbaatar:** Writing – review & editing, Methodology, Funding acquisition. **Maria Chiara Lippera:** Writing – review & editing, Software. **Snigdha Dev Roy:** Writing – review & editing, Software. **Roland Müller:** Writing – review & editing, Funding acquisition. **Jan Friesen:** Writing – review & editing, Writing – original draft, Methodology, Funding acquisition, Conceptualization.

Declaration of competing interest

The authors declare that they have no known competing financial interests or personal relationships that could have appeared to influence the work reported in this paper.

Acknowledgements

This work was supported by the European Union's Horizon H2020 projects WATERUN and MULTISOURCE (101060922 & 101003527). The scientific results have been computed at the High-Performance Computing (HPC) Cluster EVE, a joint effort of both the Helmholtz Centre for Environmental Research - UFZ and the German Centre for Integrative Biodiversity Research (iDiv) Halle-Jena-Leipzig. We thank the administration and support staff of EVE for keeping the system running and supporting us with our scientific computing needs.

Supplementary materials

Supplementary material associated with this article can be found, in the online version, at doi:10.1016/j.wroa.2025.100466.

Data availability

Data will be made available on request.

References

Angel, S., 2023. Urban expansion: theory, evidence and practice. Build. Cities 4. https://doi.org/10.5334/bc.348.

Bach, P.M., Kuller, M., McCarthy, D.T., Deletic, A., 2020. A spatial planning-support system for generating decentralised urban stormwater management schemes. Sci. Total Environ. 726, 138282. https://doi.org/10.1016/j.scitotenv.2020.138282.

Beven, K., Binley, A., 1992. The future of distributed models: model calibration and uncertainty prediction. Hydrol. Process. 6, 279–298. https://doi.org/10.1002/hyp.3360060305.

Beven, K.J., Kirkby, M.J., 1979. A physically based, variable contributing area model of basin hydrology /un modèle à base physique de zone d'appel variable de l'hydrologie du bassin versant. Hydrol. Sci. Bull. 24, 43–69. https://doi.org/10.1080/02626667909491834.
Blumensaat, F., Bloem, S., Ebi, C., Disch, A., Förster, C., Maurer, M., Rodriguez, M., Rieckermann, J., 2022a. UWO - accompanying data (2019 to 2021). https://doi.org/10.25678/000991.
Blumensaat, F., Bloem, S., Ebi, C., Disch, A., Förster, C., Maurer, M., Rodriguez, M., Rieckermann, J., 2022b UWO - field observations (2019 to 2021). https://doi.org/10.25678/00091Y.
Blumensaat, F., Bloem, S., Ebi, C., Disch, A., Förster, C., Rodriguez, M., Maurer, M., Rieckermann, J., 2023a. The UWO dataset: long-term data from a real-life field laboratory to better understand urban hydrology at small spatiotemporal scales. https://doi.org/10.31224/3208.
Blumensaat, F., Blöm, S., Ebi, C., Disch, A., Förster, C., Maurer, M., Rodriguez, M., Rieckermann, J., 2023b UWO - data access (2019 to 2021). https://doi.org/10.25678/000980.
Boeing, G., 2025. Modeling and analyzing urban networks and amenities with OSMnx. Geogr. Anal. 57, 567–577. https://doi.org/10.1111/gean.70009.
Broekhuizen, I., Leonhardt, G., Marsalek, J., Viklander, M., 2020. Event selection and two-stage approach for calibrating models of green urban drainage systems. Hydrol. Earth Syst. Sci. 24, 869–885. https://doi.org/10.5194/hess-24-869-2020.
Butler, D., Digman, C.J., Makropoulos, C., Davies, J.W., 2018. Urban Drainage, 4th ed. Taylor & Francis, CRC Press, Boca Raton, Fla, USA.
Calle, E., Martínez, D., Buttiglieri, G., Corominas, L., Farreras, M., Saló-Grau, J., Vilà, P., Pueyo-Ros, J., Comas, J., 2023. Optimal design of water reuse networks in cities through decision support tool development and testing. Npj Clean Water 6, 23. https://doi.org/10.1038/s41545-023-00222-4.
Cantone, J.P., Schmidt, A.R., 2009. Potential dangers of simplifying combined sewer hydrologic/hydraulic models. J. Hydrol. Eng. 14, 596–605. https://doi.org/10.1061/(ASCE)HE.1943-5584.0000023.
Chegini, T., Li, H.-Y., 2022. An algorithm for deriving the topology of belowground urban stormwater networks. Hydrol. Earth Syst. Sci. 26, 4279–4300. https://doi.org/10.5194/hess-26-4279-2022.
Chegini, T., Li, H.-Y., Yang, Y.C.E., Blöschl, G., Leung, L.R., 2025. A scale-adaptive urban hydrologic framework: incorporating network-level storm drainage pipes representation. Water Resour. Res. 61. https://doi.org/10.1029/2024WR037268 e2024WR037268.
Conzen, M.R.G., 1960. Alnwick, Northumberland: a study in town-plan analysis. Trans. Pap. Inst. Br. Geogr iii. https://doi.org/10.2307/621094.
Dobson, B., Jovanovic, T., Alonso-Álvarez, D., Chegini, T., 2025. SWMManywhere: a workflow for generation and sensitivity analysis of synthetic urban drainage models, anywhere. Environ. Model. Softw. 186, 106358. https://doi.org/10.1016/j.envsoft.2025.106358.
Duan, Q., Sorooshian, S., Gupta, V.K., 1994. Optimal use of the SCE-UA global optimization method for calibrating watershed models. J. Hydrol. 158, 265–284. https://doi.org/10.1016/0022-1694(94)90057-4.
Duque, N., Bach, P.M., Scholten, L., Fappiano, F., Maurer, M., 2022. A simplified sanitary sewer system generator for exploratory modelling at City-scale. Water Res. 209, 117903. https://doi.org/10.1016/j.watres.2021.117903.
European Parliament and Council of the European Union, 2024. Directive (EU) 2024/3019 of the European Parliament and of the Council of 27 November 2024 concerning urban wastewater treatment (recast). OJ L 3019.
Farina, A., Di Nardo, A., Gargano, R., van der Werf, J.A., Greco, R., 2023. A simplified approach for the hydrological simulation of urban drainage systems with SWMM. J. Hydrol. 623, 129757. https://doi.org/10.1016/j.jhydrol.2023.129757.
Farina, A., Gargano, R., Greco, R., 2024. Effects of urban catchment characteristics on combined sewer overflows. Environ. Res. 244, 117945. https://doi.org/10.1016/j.envres.2023.117945.
Fowler, H.J., Lenderink, G., Prein, A.F., Westra, S., Allan, R.P., Ban, N., Barbero, R., Berg, P., Blenkinsop, S., Do, H.X., Guerreiro, S., Haerter, J.O., Kendon, E.J., Lewis, E., Schaer, C., Sharma, A., Villarini, G., Wasko, C., Zhang, X., 2021. Anthropogenic intensification of short-duration rainfall extremes. Nat. Rev. Earth Environ. 2, 107–122. https://doi.org/10.1038/s43017-020-00128-6.
Friesen, J., Khurelbaatar, G., Plaul, B., Despot, D., Van Afferden, M., Müller, R.A., Breulmann, M., 2025. Co-designing water-sensitive suburbs through blue-green infrastructure planning by research, municipal and housing association partners. In: Lens, P.N.L., Bui, X.-T. (Eds.), Nature-Based Solutions for Urban Sustainability. IWA Publishing, pp. 175–190. https://doi.org/10.2166/9781789065015_0175.
German Aerospace Center, 2023. World settlement footprint (WSF) 2019 - Sentinel-1/2 - global. https://doi.org/10.15489/TWG5XSNQUW84.
Ghosh, I., Hellweger, F.L., 2012. Effects of spatial resolution in urban hydrologic simulations. J. Hydrol. Eng. 17, 129–137. https://doi.org/10.1061/(ASCE)HE.1943-5584.0000405.
Goldstein, A., Romano, Foti, Foti, R., Franco, Montalto, Montalto, F., 2016. Effect of spatial resolution in modeling stormwater runoff for an urban block. J. Hydrol. Eng. 21, 06016009. https://doi.org/10.1061/(asce)he.1943-5584.0001377.
Gupta, H.V., Kling, H., Yilmaz, K.K., Martinez, G.F., 2009. Decomposition of the mean squared error and NSE performance criteria: implications for improving hydrological modelling. J. Hydrol. 377, 80–91. https://doi.org/10.1016/j.jhydrol.2009.08.003.
Hagberg, A.A., Schult, D.A., Swart, P.J., 2008. Exploring network structure, dynamics, and function using NetworkX. In: Varoquaux, G., Vaught, T., Millman, J. (Eds.), Proceedings of the 7th Python in Science Conference. Pasadena, CA USA, pp. 11–15.
Herman, J., Usher, W., 2017. SALib: an open-source Python library for sensitivity analysis. J. Open Source Softw. 2, 97. https://doi.org/10.21105/joss.00097.
Houska, T., Kraft, P., Chamorro-Chavez, A., Breuer, L., 2015. SPOTting model parameters using a ready-made Python package. PLOS ONE 10, e0145180. https://doi.org/10.1371/journal.pone.0145180.
Hwang, F.K., Richards, D.S., 1992. Steiner tree problems. Networks 22, 55–89. https://doi.org/10.1002/net.3230220105.
James, W., 2000. Rules For Responsible Modeling, 4th ed. CHI Press, Guelph, Ontario.
Ji, S., Qiuwen, Z., 2015. A GIS-based subcatchments Division approach for SWMM. Open Civ. Eng. J. 9, 515–521. https://doi.org/10.2174/1874149501509010515.
Joshi, P., Leitão, J.P., Maurer, M., Bach, P.M., 2021. Not all SuDS are created equal: impact of different approaches on combined sewer overflows. Water Res. 191, 116780. https://doi.org/10.1016/j.watres.2020.116780.
Khurelbaatar, G., van Afferden, M., Ueberham, M., Stefan, M., Geyler, S., Müller, R.A., 2021. Management of urban stormwater at block-level (MUST-B): A new approach for potential analysis of decentralized stormwater management systems. Water 13, 378. https://doi.org/10.3390/w13030378.
Knoben, W.J.M., Freer, J.E., Woods, R.A., 2019. Technical note: inherent benchmark or not? Comparing Nash–Sutcliffe and Kling–Gupta efficiency scores. Hydrol. Earth Syst. Sci. 23, 4323–4331. https://doi.org/10.5194/hess-23-4323-2019.
Krebs, G., Kokkonen, T., Valtanen, M., Setälä, H., Koivusalo, H., 2014. Spatial resolution considerations for urban hydrological modelling. J. Hydrol. 512, 482–497. https://doi.org/10.1016/j.jhydrol.2014.03.013.
Kuller, M., Bach, P.M., Ramirez-Lovering, D., Deletic, A., 2017. Framing water sensitive urban design as part of the urban form: a critical review of tools for best planning practice. Environ. Model. Softw. 96, 265–282. https://doi.org/10.1016/j.envsoft.2017.07.003.
Kuller, M., Farrelly, M., Marthanty, D.R., Deletic, A., Bach, P.M., 2022. Planning support systems for strategic implementation of nature-based solutions in the global south: current role and future potential in Indonesia. Cities 126, 103693. https://doi.org/10.1016/j.cities.2022.103693.
Lippera, M.C., Khurelbaatar, G., Despot, D., Kouyi, G.L., Rizzo, A., Friesen, J., 2025. Spatial-economic scenarios to increase resilience to urban flooding. Water Res. X 26, 100284. https://doi.org/10.1016/j.wroa.2024.100284.
Martin-Mikle, C.J., de Beurs, K.M., Julian, J.P., Mayer, P.M., 2015. Identifying priority sites for low impact development (LID) in a mixed-use watershed. Landsc. Urban Plan. 140, 29–41. https://doi.org/10.1016/j.landurbplan.2015.04.002.
MeteoSwiss, 2024. MeteoSwiss IDAWEB: 10-minute precipitation for Station Kloten, 1988–2023 (order 124656). IDAWEB MeteoSwiss Data Portal.
Montoya-Coronado, V.A., Tedoldi, D., Castebrunet, H., Molle, P., Lipeme Kouyi, G., 2024. Data-driven methodological approach for modeling rainfall-induced infiltration effects on combined sewer overflow in urban catchments. J. Hydrol. 632, 130834. https://doi.org/10.1016/j.jhydrol.2024.130834.
Moudon, A.V., 1997. Urban morphology as an emerging interdisciplinary field. Urban Morphol. 1, 3–10. https://doi.org/10.51347/jum.v1i1.4047.
Oliveira, V., 2024. Urban form and the socioeconomic and environmental dimensions of cities. J. Urban. Int. Res. Placemaking Urban Sustain. 17, 1–23. https://doi.org/10.1080/17549175.2021.2011378.
Petrie, B., 2021. A review of combined sewer overflows as a source of wastewater-derived emerging contaminants in the environment and their management. Environ. Sci. Pollut. Res. 28, 32095–32110. https://doi.org/10.1007/s11356-021-14103-1.
Phillips, P.J., Chalmers, A.T., Gray, J.L., Kolpin, D.W., Foreman, W.T., Wall, G.R., 2012. Combined sewer overflows: an environmental source of hormones and wastewater micropollutants. Environ. Sci. Technol. 46, 5336–5343. https://doi.org/10.1021/es3001294.
Pichler, M., 2025. swmm_api: a Python package for automation, customization, and visualization in SWMM-based Urban drainage modeling. Water (Basel) 17, 1373. https://doi.org/10.3390/w17091373.
Pichler, M., König, A.W., Reinstaller, S., Muschalla, D., 2024. Fully automated simplification of urban drainage models on a city scale. Water Sci. Technol., wst2024337 https://doi.org/10.2166/wst.2024.337.
Quaranta, E., Fuchs, S., Jan Liefting, H., Schellart, A., Pistocchi, A., 2022. A hydrological model to estimate pollution from combined sewer overflows at the regional scale: application to Europe. J. Hydrol. Reg. Stud. 41, 101080. https://doi.org/10.1016/j.ejrh.2022.101080.
Rauch, W., Urich, C., Bach, P.M., Rogers, B.C., de Haan, F.J., Brown, R.R., Mair, M., McCarthy, D.T., Kleidorfer, M., Sitzenfrei, R., Deletic, A., 2017. Modelling transitions in urban water systems. Water Res. 126, 501–514. https://doi.org/10.1016/j.watres.2017.09.039.
Reyes-Silva, J.D., Zischg, J., Klinkhamer, C., Rao, P.S.C., Sitzenfrei, R., Krebs, P., 2020. Centrality and shortest path length measures for the functional analysis of urban drainage networks. Appl. Netw. Sci. 5, 1–14. https://doi.org/10.1007/s41109-019-0247-8.
Rodriguez, M., Cavadini, G.B., Cook, L.M., 2024. Do baseline assumptions alter the efficacy of green stormwater infrastructure to reduce combined sewer overflows? Water Res. 121284. https://doi.org/10.1016/j.watres.2024.121284.
Rossman, L.A., 2017. Storm Water Management Model Reference Manual Volume II – Hydraulics (No. EPA/600/R-17/111). U.S. Environmental Protection Agency., Washington, DC.
Rossman, L.A., 2010. Storm Water Management Model (SWMM) User's Manual, Version 5.1 (Report). U.S. Environmental Protection Agency, Office of Research and Development, National Risk Management Research Laboratory, Cincinnati, OH.
Saltelli, A., 2002. Making best use of model evaluations to compute sensitivity indices. Comput. Phys. Commun. 145, 280–297. https://doi.org/10.1016/S0010-4655(02)00280-1.
Sanne, M., Khurelbaatar, G., Despot, D., Afferden, M.van, Friesen, J., 2024. Pysewer: a Python library for sewer network generation in data scarce regions. J. Open Source Softw. 9, 6430. https://doi.org/10.21105/joss.06430.

Schilling, J., Tränckner, J., 2022. Generate_SWMM_inp: an open-source QGIS plugin to import and export model input files for SWMM. Water (Basel) 14, 2262. https://doi.org/10.3390/w14142262.

Si, Q., Brito, H.C., Alves, P.B.R., Pavao-Zuckerman, M.A., Rufino, I.A.A., Hendricks, M.D., 2024. GIS-based spatial approaches to refining urban catchment delineation that integrate stormwater network infrastructure. Discov. Water 4, 24. https://doi.org/10.1007/s43832-024-00083-z.

Siksna, A., 1997. The evolution of block size and form in North American and Australian city centres. Urban Morphol 1, 19–33. https://doi.org/10.51347/jum.v1i1.4048.

Sobol′, I.M., 2001. Global sensitivity indices for nonlinear mathematical models and their Monte Carlo estimates. Math. Comput. Simul., The Second IMACS Seminar on Monte Carlo Methods 55, 271–280. https://doi.org/10.1016/S0378-4754(00)00270-6.

Staufer, P., Scheidegger, A., Rieckermann, J., 2012. Assessing the performance of sewer rehabilitation on the reduction of infiltration and inflow. Water Res. 46, 5185–5196. https://doi.org/10.1016/j.watres.2012.07.001.

Stone, M., 1974. Cross-validatory choice and assessment of statistical predictions. J. R. Stat. Soc. Ser. B Methodol. 36, 111–133. https://doi.org/10.1111/j.2517-6161.1974.tb00994.x.

Tibbetts, J., 2005. Combined sewer systems: down, dirty, and out of date. Environ. Health Perspect. 113, A464–A467. https://doi.org/10.1289/ehp.113-a464.

United States Congress, 2019. Water Infrastructure Improvement Act, stat.

United States Environmental Protection Agency, 1994. Combined Sewer Overflow (CSO) Control Policy: Final Policy. Federal Register. U.S. Environmental Protection Agency, Washington, DC.

Virtanen, P., Gommers, R., Oliphant, T.E., Haberland, M., Reddy, T., Cournapeau, D., Burovski, E., Peterson, P., Weckesser, W., Bright, J., van der Walt, S.J., Brett, M., Wilson, J., Millman, K.J., Mayorov, N., Nelson, A.R.J., Jones, E., Kern, R., Larson, E., Carey, C.J., Polat, İ., Feng, Y., Moore, E.W., VanderPlas, J., Laxalde, D., Perktold, J., Cimrman, R., Henriksen, I., Quintero, E.A., Harris, C.R., Archibald, A.M., Ribeiro, A. H., Pedregosa, F., van Mulbregt, P., 2020. SciPy 1.0: fundamental algorithms for scientific computing in Python. Nat. Methods 17, 261–272. https://doi.org/10.1038/s41592-019-0686-2.

Wright, T.J., Liu, Y., Carroll, N.J., Ahiablame, L.M., Engel, B.A., 2016. Retrofitting LID practices into existing neighborhoods: is it worth it? Environ. Manage. 57, 856–867. https://doi.org/10.1007/s00267-015-0651-5.